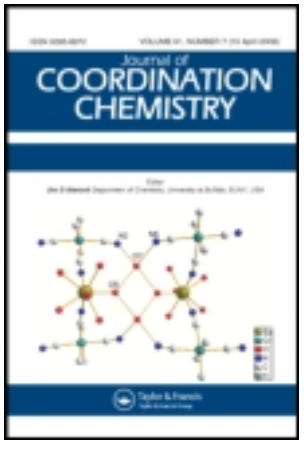

Journal of Coordination Chemistry
Publication details, including instructions for authors and subscription information:
http://www.tandfonline.com/loi/gcoo20

The synthesis, molecular, crystal, and electronic structures of $[ReBr_2(O)(OCH_3)(PPh_3)_2]$

S. Michalik [a], J.G. Małecki [b], R. Kruszynski [c], V. Kozik [d], J. Kusz [e] & M. Krompiec [a]

[a] Department of Inorganic and Coordination Chemistry, Institute of Chemistry, University of Silesia, 9th Szkolna St., 40-006 Katowice, Poland

[b] Department of Crystallography, Institute of Chemistry, University of Silesia, ul. Szkolna 9, 40-006, Katowice, Poland

[c] Department of X-ray Crystallography and Crystal Chemistry, Institute of General and Ecological Chemistry, Technical University of Łódź, 116 Żeromski St., 90-924 Łódź, Poland

[d] Department of Organic Synthesis Chemistry, Institute of Chemistry, University of Silesia, ul. Szkolna 9, 40-006 Katowice, Poland

[e] Institute of Physics, University of Silesia, 4th Uniwersytecka St., 40-006 Katowice

Published online: 01 Jul 2011.

To cite this article: S. Michalik, J.G. Małecki, R. Kruszynski, V. Kozik, J. Kusz & M. Krompiec (2011) The synthesis, molecular, crystal, and electronic structures of $[ReBr_2(O)(OCH_3)(PPh_3)_2]$, Journal of Coordination Chemistry, 64:12, 2202-2213, DOI: 10.1080/00958972.2011.591930

To link to this article: http://dx.doi.org/10.1080/00958972.2011.591930

Journal of Coordination Chemistry
Vol. 64, No. 12, 20 June 2011, 2202–2213

The synthesis, molecular, crystal, and electronic structures of $[ReBr_2(O)(OCH_3)(PPh_3)_2]$

S. MICHALIK*†, J.G. MAŁECKI‡, R. KRUSZYNSKI§, V. KOZIK¶, J. KUSZ‖ and M. KROMPIEC†

†Department of Inorganic and Coordination Chemistry, Institute of Chemistry, University of Silesia, 9th Szkolna St., 40-006 Katowice, Poland
‡Department of Crystallography, Institute of Chemistry, University of Silesia, ul. Szkolna 9, 40-006, Katowice, Poland
§Department of X-ray Crystallography and Crystal Chemistry, Institute of General and Ecological Chemistry, Technical University of Łódź, 116 Żeromski St., 90-924 Łódź, Poland
¶Department of Organic Synthesis Chemistry, Institute of Chemistry, University of Silesia, ul. Szkolna 9, 40-006 Katowice, Poland
‖Institute of Physics, University of Silesia, 4th Uniwersytecka St., 40-006 Katowice

(*Received 19 March 2011; in final form 2 May 2011*)

$[ReBr_2(O)(OCH_3)(PPh_3)_2]$ has been obtained in the reaction of $[ReBr_3O(PPh_3)_2]$ or $[ReBr_2(\eta^2\text{-}N_2COPh\text{-}N',O)(PPh_3)_2]$ with an excess of methanol. $[ReBr_2O(OMe)(PPh_3)_2]$ crystallizes in the triclinic space group *P*-1. The complex was characterized by infrared, UV-Vis, and ^1H NMR spectra. The electronic structure of the obtained compound has been calculated using the DFT/TD–DFT method.

Keywords: Rhenium; X-ray structure; Electronic structure; DFT calculations

1. Introduction

Studies of coordination chemistry of rhenium have increased due to therapeutic applications in nuclear medicine. Rhenium(V) complexes as radiopharmaceuticals for therapy and diagnosis have received attention because of their suitable radionuclear properties, i.e., ^{186}Re: $E_{max} = 1.1\,MeV$ for β-emission and $E_{max} = 0.137\,MeV$ for γ-emission with $t_{1/2} = 90.6$ h, ^{188}Re: $E_{max} = 2.1\,MeV$ for β-emission and $E_{max} = 0.155\,MeV$ for γ-emission with $t_{1/2} = 17\,h$ [1–5]. Another area of major interest for rhenium(V) compounds is their application as catalysts. Oxo rhenium(V) complexes catalyze oxygen-transfer reactions [6], reduction of carbonyl groups [7], sulfide oxidation [8], radical polymerization of styrene [9], catalytic oxidations [10], olefination [11], etc.

This article presents the synthesis, crystal, molecular, and electronic structures and the spectroscopic characterization of $[ReBr_2O(OMe)(PPh_3)_2]$. This complex is similar to

*Corresponding author. Email: smich1@wp.pl

Journal of Coordination Chemistry
ISSN 0095-8972 print/ISSN 1029-0389 online © 2011 Taylor & Francis
DOI: 10.1080/00958972.2011.591930

well-known oxo rhenium(V) complexes such as the ethoxy analog $[ReBr_2(O)(OEt)(PhP_3)_2]$ [12] and chloro analog $[ReCl_2(O)(OMe)(PPh_3)_2]$ [13] which were not studied with DFT.

The electronic structure of the obtained compound has been calculated using the DFT/TD–DFT method. Currently, density functional theory (DFT) is commonly used to examine the electronic structure of transition metal complexes. It meets with the requirements of being accurate, easy to use, and fast enough to allow the study of relatively large molecules of transition metal complexes [14, 15]. Recent calculations with the TDDFT method for open- and closed-shell 5 d-metal complexes (including rhenium complexes) have also supported that TDDFT is applicable for such systems, giving good assignment of experimental spectra [16–18].

2. Experimental

Ammonium perrhenate and triphenylphosphine were purchased from Aldrich Chemical and methanol was purchased from Fluka AG and used without purification. $[ReBr_3O(PPh_3)_2]$ and $[ReBr_2(\eta^2\text{-}N_2COPh\text{-}N',O)(PPh_3)_2]$ were prepared according to the literature methods [19, 20].

2.1. *Synthesis of $[ReBr_2(O)(OCH_3)(PPh_3)_2]$*

Method A: a suspension of $[ReBr_3O(PPh_3)_2]$ (200 mg, 0.218 mmol) in 50 mL MeOH (not dried prior to use) was refluxed for three days in air. The brown crystalline precipitate was collected by filtration and crystals suitable for X-ray structure determination were obtained by recrystallization from a mixture of chloroform and methanol. Yield 65%. Infrared (IR) (KBr), selected bands, cm^{-1}: 3054 m, br ν_{as}(CH) and 2970 w ν_s(CH), 1481 s and 1433 s ν(PPh), 1093 s ν(OMe), 910 s ν(Re=O), 747 s and 692 s ν(PPh), 521 s ν(Re–OMe). UV-Vis (acetonitrile), 523, 372, 362, 273, 211. ^{1}H NMR ($CDCl_3$), d: 7.75–7.39 (m, 30 H, PPh_3), 2.26 (s, 3 H, OMe). $^{31}P\{^1H\}$ NMR ($CDCl_3$), d: 35.59 (s). Anal. Calcd for $C_{37}H_{33}Br_2O_2P_2Re$ (%): C, 48.43; H, 3.62. Found (%): C, 48.45; H, 3.63.

Method B: a green suspension of $[ReBr_2(\eta^2\text{-}N_2COPh\text{-}N',O)(PPh_3)_2]$ (250 mg, 0.249 mmol) in 60 mL MeOH (not dried prior to use) was refluxed for 2 days in air to produce a brown cloudy solution. The brown crystalline precipitate was collected by filtration. X-ray quality crystals were obtained by slow evaporation of the reaction filtrate at room temperature. Yield 22%.

2.2. *Physical measurements and DFT calculations*

IR spectra were recorded on a Perkin-Elmer spectrophotometer from 4000 to 450 cm^{-1} using KBr pellets. Electronic spectra were measured on a Lab Alliance UV-Vis 8500 spectrophotometer from 600 to 180 nm in acetonitrile. ^{1}H and ^{31}P NMR spectra were obtained at room temperature in $CDCl_3$ using a Bruker 400 spectrometer. Elemental analyses (C, H, N) were performed on a Perkin-Elmer CHNS-2400 analyzer. Electrochemical measurements were carried out using an Eco Chemie Autolab PGSTAT128n potentiostat. Platinum wire (diam. 1 mm), platinum coil, and silver wire as working, auxiliary, and reference electrode, respectively, were used. Potentials are

referenced with respect to ferrocene, which served as the internal standard. Cyclic voltammetry (100 $mV\,s^{-1}$) experiments were conducted in a standard one-compartment cell, in dichloromethane (Carlo Erba, HPLC grade), under argon. Bu_4NPF_6 (Aldrich, 99%, recrystallized from isopropanol and dried in vacuum at 160°C) was used as the supporting electrolyte (0.2 $mol\,L^{-1}$ in CH_2Cl_2).

Calculations were carried out using the Gaussian09 program [21]. The DFT/B3LYP method [22, 23] was used for the geometry optimization and electronic structure determination. Electronic spectra were calculated by the TD-DFT method [24] with the use of the CAM-B3LYP functional [25]. Calculations were performed using the Lanl2dz basis set [26] on rhenium and bromine and polarization functions for all other atoms: 6–31 G** for chlorine, carbon, nitrogen, oxygen and 6-31 G for hydrogen. The PCM solvent model was used in the Gaussian calculations with methanol as solvent. Natural bond orbital (NBO) calculations were performed with the NBO code included in Gaussian09. GaussSum 2.2 [27] was used to calculate group contributions to the molecular orbitals and to prepare the partial density of states (DOS) and overlap population density of states (OPDOS) spectra. The contribution of a group to a molecular orbital was calculated using the Mulliken population analysis. PDOS and OPDOS spectra were created by convoluting the molecular orbital information with Gaussian curves of unit height and FWHM of 0.3 eV.

2.3. *Crystal structure determination and refinement*

Crystals of $[ReBr_2(O)(OCH_3)(PPh_3)_2]$ suitable for X-ray structure determination were obtained by recrystallization from a mixture of chloroform and methanol. A red-brown crystal was mounted on a KM-4-CCD automatic diffractometer equipped with a CCD detector and used for data collection. X-ray intensity data were collected with graphite-monochromated Mo-Kα radiation ($\lambda = 0.71073$ Å) at room temperature with ω scan mode. A 25 s exposure time was used and the Ewald sphere was collected up to $2\theta = 50.06°$. The unit cell parameters were determined from least-squares refinement of the setting angles of 11,079 strongest reflections. Details concerning crystal data and refinement for $[ReBr_2(O)(OCH_3)(PPh_3)_2]$ are given in table 1. Lorentz, polarization, and numerical absorption corrections [28] were applied. The structure was solved by the Patterson method and subsequently completed by difference Fourier recycling. All non-hydrogen atoms were refined anisotropically using full-matrix, least-squares. All hydrogens were found on difference Fourier synthesis and refined as ''riding'' on their parent carbons with geometry idealization after each cycle and assigned isotropic temperature factors equal 1.2 (non-methyl) or 1.5 (methyl) times the value of the parent carbon equivalent temperature factor. The methyl group was allowed to rotate about their local three-fold axis. SHELXS97 [29], SHELXL97 [30], and SHELXTL [31] were used for all calculations.

3. Results and discussion

$[ReBr_2(O)(OCH_3)(PPh_3)_2]$ was obtained from direct reactions of $[ReBr_3O(PPh_3)_2]$ or $[ReBr_2(\eta^2\text{-}N_2COPh\text{-}N',O)(PPh_3)_2]$ with methanol. The complex crystallizes in the

Table 1. Crystal data and structure refinement details of $[ReBr_2(O)(OCH_3)(PPh_3)_2]$.

Empirical formula	$C_{37}H_{33}Br_2O_2P_2Re$
Formula weight	917.59
Temperature (K)	295(1)
Crystal system	Triclinic
Space group	*P*-1
Unit cell dimensions (Å, °)	
a	11.2906(6)
b	11.7621(8)
c	14.2619(8)
α	87.350(5)
β	80.744(5)
γ	69.757(6)
Volume (Å^3), *Z*	1753.78(18), 2
Calculated density (Mg m^{-3})	1.738
Absorption coefficient (mm^{-1})	5.865
F(000)	892
Crystal dimensions (mm^3)	$0.24 \times 0.19 \times 0.02$
θ range for data collection (°)	3.11 to 25.03
Index ranges	$-11 \le h \le 13$; $-13 \le k \le 13$; $-16 \le l \le 16$
Reflections collected	11,079
Independent reflections	6006 [$R_{(int)} = 0.0317$]
Data/restraints/parameters	6006/0/398
Goodness-of-fit on F^2	0.936
Final *R* indices [$I > 2\sigma(I)$]	$R_1 = 0.0309$; $wR_2 = 0.0669$
R indices (all data)	$R_1 = 0.0472$; $wR_2 = 0.0701$
Largest difference peak and hole (eÅ^{-3})	1.451 and −1.137

triclinic space group *P*-1 and its crystal structure is composed of discrete monomers with all atoms located in general positions. The molecular structure is shown in figure 1. $[ReBr_2(O)(OCH_3)(PPh_3)_2]$ is stable in the solid state and in solutions of common solvents, for example, CH_2Cl_2, $CHCl_3$, or C_6H_6.

The IR spectrum also exhibits characteristic strong ν(OMe) and ν(Re=O) bands at 1094 and 946 cm^{-1}, respectively, in agreement with other methoxy- and/or oxo rhenium complexes [32–34]. Also, the complex contains triphenylphosphine and thus shows the characteristic pair of bands at approximately 1433 and 1481 cm^{-1} and, typically, the lower frequency band is more intense [35].

The ^{1}H NMR spectrum shows expected resonances for the coordinated PPh_3 and OMe [34, 36], while the singlet in the $^{31}P\{^1H\}$ spectrum is consistent with *trans* coordination of the two triphenylphosphines.

The molecular structure exhibits a distorted octahedral coordination geometry about the rhenium centre with two *trans* PPh_3 molecules minimizing steric congestion. The oxo, methoxy, and two *trans* bromides are in the equatorial positions. Selected bond lengths and angles are summarized in table 2.

The Re–O(1) bond length of 1.694(3) Å is in agreement with normal Re–O_{oxo} bond distances (*ca* 1.67–1.70 Å) [34, 37, 38] in six-coordinate monooxorhenium complexes. The Re–O(2) distance of 1.898(4) Å is also unexceptional for Re compounds with methoxy [34, 39]. The major deviation from octahedral geometry is the O(1)–Re–O(2) angle of 176.12(15)°, whereas the other bond angles are relatively close to the idealized 90° and 180°. Thus, both triphenylphosphines and bromide are bound almost linearly

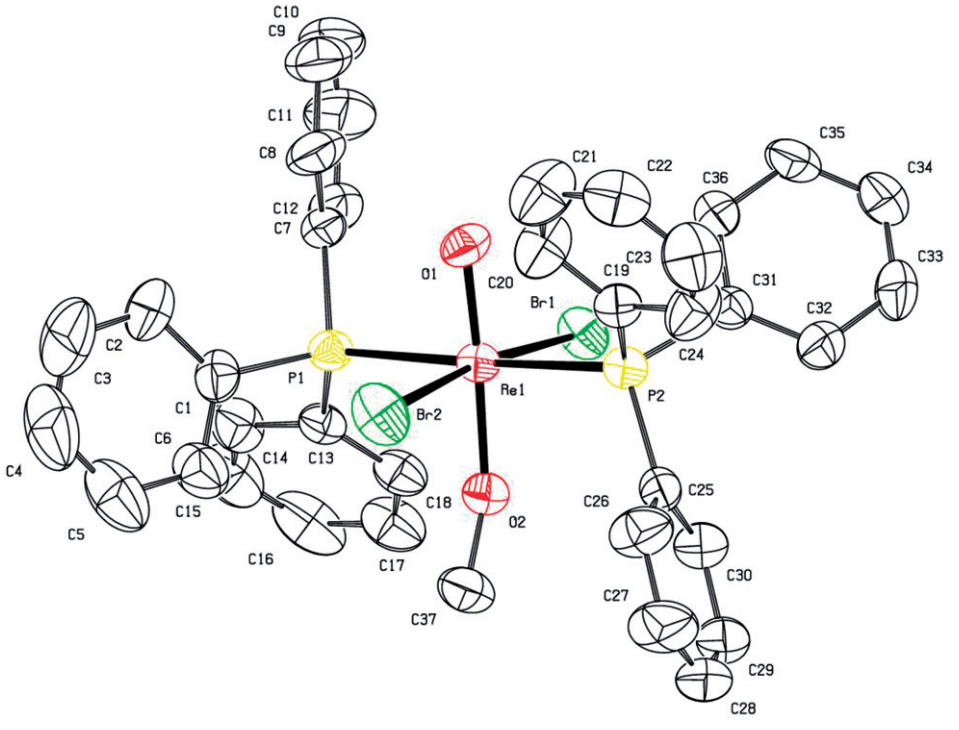

Figure 1. ORTEP drawing of $[ReBr_2(O)(OCH_3)(PPh_3)_2]$ with 50% probability displacement ellipsoids. Hydrogens are omitted for clarity.

Table 2. Selected bond lengths (Å) and angles (°) for $[ReBr_2(O)(OCH_3)(PPh_3)_2]$.

	Exp.	Calcd
Re(1)–O(1)	1.694(3)	1.7762
Re(1)–O(2)	1.870(3)	1.9588
Re(1)–P(1)	2.5281(14)	2.6099
Re(1)–P(2)	2.5229(14)	2.5856
Re(1)–Br(1)	2.5421(6)	2.6190
Re(1)–Br(2)	2.5639(6)	2.6513
P(1)–Re(1)–P(2)	177.71(4)	171.94
P(1)–Re(1)–O(1)	88.64(12)	86.82
P(1)–Re(1)–O(2)	90.17(11)	89.99
O(1)–Re(1)–O(2)	176.12(15)	165.87
P(2)–Re(1)–O(1)	89.08(12)	86.04
P(2)–Re(1)–O(2)	92.11(11)	100.06
O(1)–Re(1)–Br(1)	95.07(12)	100.10
O(1)–Re(1)–Br(2)	91.97(12)	86.07
O(2)–Re(1)–Br(1)	88.63(10)	90.35
O(2)–Re(1)–Br(2)	84.38(10)	82.87
Br(1)–Re(1)–Br(2)	172.63(2)	169.51
P(1)–Re(1)–Br(1)	90.16(3)	87.98
P(2)–Re(1)–Br(1)	90.01(3)	87.24
P(1)–Re(1)–Br(2)	92.18(4)	101.20
P(2)–Re(1)–Br(2)	87.93(3)	84.43

Table 3. Hydrogen-bonding geometry for [$ReBr_2(O)(OCH_3)(PPh_3)_2$].

D–H···A	H···A	D···A	∠(DHA)
C8–H8···O1	2.55	2.9140	104.00
C10–H10···Br1#1	2.92	3.8302	166.00
C18–H18···Br1	2.77	3.5026	136.00
C20–H20···O1	2.42	3.1726	138.00

#1: $1-x, -y, 1-z$.

(i.e., P(1)–Re–P(2) 177.71(4)° and Br(1)–Re–Br(2) 172.63(2)° with average Re–P and Re–Br distances of 2.5255(14) and 2.5536(7) Å, respectively. The Re–P and Re–Br bond distances fall within the normal range in six-coordinate rhenium complexes [40].

The structure is stabilized by multiple weak intra- and intermolecular hydrogen bonds [41, 42] with data given in table 3. The packing diagram of [$ReBr_2(O)(OCH_3)(PPh_3)_2$] is depicted in figure 2. Electrochemical properties of [$ReOBr_2(OMe)(PPh_3)_2$] in CH_2Cl_2 solution were studied by cyclic voltammetry. No reduction peaks were found in the available potential window. Two irreversible oxidation processes were detected, with peak potentials at 0.81 and 1.06 V *versus* Fc (Supplementary material). The first process corresponds to a Re^{V}/Re^{VI} oxidation (probably coupled to a secondary chemical transformation) and is slightly (about 80 mV) shifted to less positive potentials relative to the oxidation potential of a [$Re^{V}OBr_2$(NNO-chelate)] complex described by Wei *et al.* [43], and lies within the range of oxidation potentials of [$Re^{(V)}$(diolate)($\mu^3-B(pz)_4$)] complexes studied by Nunes *et al.* [44]. The second anodic peak may be attributed to a Re^{VI}/Re^{VII} oxidation.

3.1. *Electronic structure and spectrum*

To gain insight into the electronic structures and bonding properties of the complex, DFT calculations were carried out. Before the calculations of electronic structures of the complexes, their geometry was optimized in singlet state using the B3LYP functional. From the data collected in table 2, one may see that the bond lengths are maximally elongated by ~0.09 Å in the calculated gas phase structures. For the optimized angles, the maximum differences from the experimental values in O(1)–Re(1)–O(2) and P(1)–Re(1)–Br(2) are 10.25° and 9.02°. Nevertheless, the calculated and experimental IR spectra of the complex are in good agreement as one can see in figure 3.

Among the occupied MOs of the complexes, the largest numbers constitute orbitals of the triphenylphosphine ligands which are not relevant for the discussion. The d_{yz}, d_{xy}, and d_{zx} orbitals of rhenium contribute to the HOMO (38%), HOMO–18 (33%), and HOMO–19 (14%). These molecular orbitals are mixed with p orbitals of the bromides. The $d_{x^2-y^2}$ and d_{z^2} orbitals are visible in the LUMO (60%) and LUMO + 1 (62%) with an anti-bonding admixture of p oxo orbitals. Table 4 presents the composition of frontier molecular orbitals of the complex. The partial DOS and OPDOS in terms of the Mulliken population analysis were calculated using the GaussSum program. They provide a pictorial representation of the MO compositions and their contributions to chemical bonding. The DOS diagram for the complex is shown in figure 4. The DOS plot mainly presents the composition of the fragment

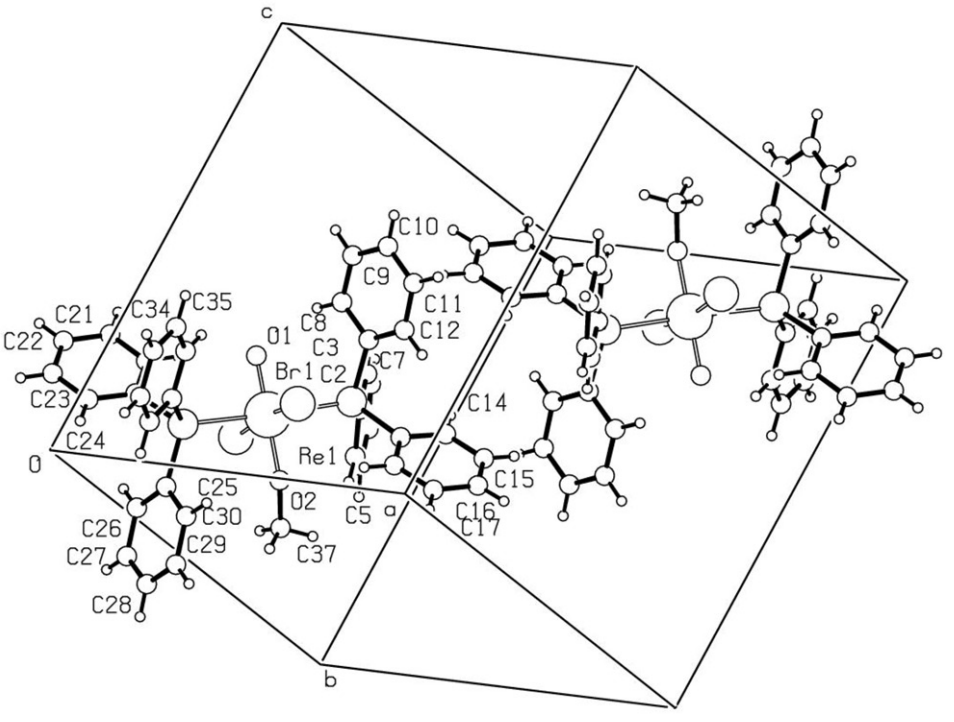

Figure 2. The packing diagram of $[ReBr_2(O)(OCH_3)(PPh_3)_2]$.

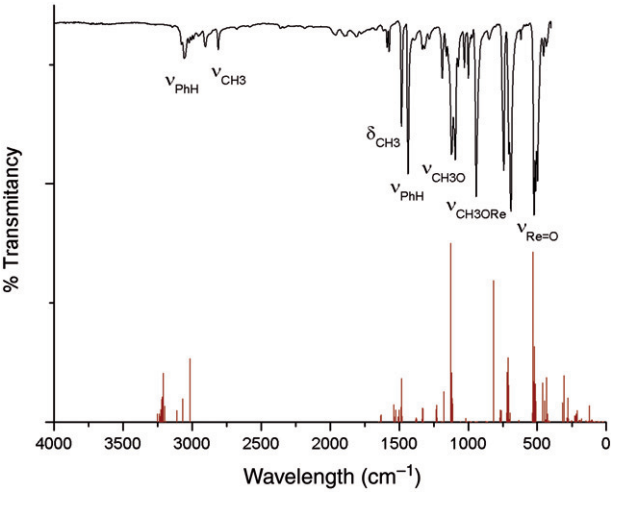

Figure 3. IR spectrum of $[ReBr_2(O)(OCH_3)(PPh_3)_2]$.

orbitals contributing to the molecular orbitals. As may be seen from the DOS plots, the HOMO has d_{Re} and p_{Br} character and the LUMO and LUMO + 1 are composed of d rhenium and π^* orbitals of the oxo. The PPh_3 ligands play a role in lower occupied and higher virtual molecular orbitals.

Table 4. Composition of frontier molecular orbitals of [$ReBr_2(O)(OCH_3)(PPh_3)_2$].

	eV	Re	Br	O	OCH_3	PPh_3
L + 10	−0.2	4	2	1	0	94
L + 9	−0.31	3	2	0	0	95
L + 8	−0.39	8	4	0	0	88
L + 7	−0.44	7	4	1	0	87
L + 6	−0.52	3	2	0	0	95
L + 5	−0.68	10	6	0	0	83
L + 4	−0.76	3	2	0	0	95
L + 3	−0.82	3	2	0	0	95
L + 2	−1.41	33	14	0	0	53
L + 1	−2.2	62	4	21	12	2
LUMO	−2.72	60	2	25	9	4
HOMO	−5.24	38	49	1	2	10
H-1	−6.01	2	28	3	4	63
H-2	−6.1	2	83	2	4	8
H-3	−6.26	5	62	2	4	27
H-4	−6.5	4	45	0	4	48
H-5	−6.61	6	35	3	2	54
H-6	−6.69	3	26	3	13	56
H-7	−6.73	0	5	0	1	94
H-8	−6.77	1	1	0	1	97
H-9	−6.82	2	10	0	5	83
H-10	−6.9	2	3	2	6	87
H-11	−6.94	1	11	2	1	85
H-12	−6.97	1	13	0	2	83
H-13	−7.03	3	6	1	0	90
H-14	−7.07	1	3	0	4	91
H-15	−7.13	0	1	0	1	98
H-16	−7.32	1	3	0	3	93
H-17	−7.42	5	13	7	26	49
H-18	−7.79	33	28	3	17	20
H-19	−8.05	14	24	13	44	6

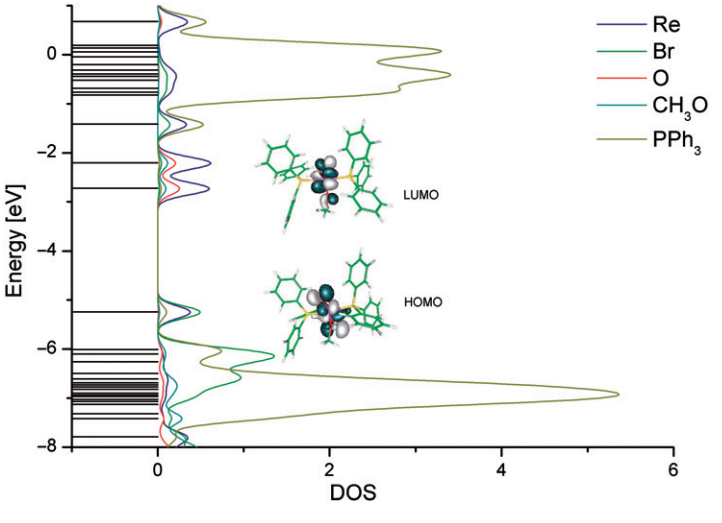

Figure 4. The DOS diagram for [$ReBr_2(O)(OCH_3)(PPh_3)_2$].

The OPDOS gives an indication of the bonding, non-bonding, and anti-bonding characteristics with respect to the particular fragments. A positive value in the OPDOS plot means a bonding interaction, while a negative value represents an anti-bonding interaction, and a near zero value indicates a non-bonding interaction. At the same time, analysis of the OPDOS diagram allows us to determine the donor–acceptor properties of the ligands. From figure 5, it may be concluded that methoxy has small σ-donor properties.

On the electronic spectrum of the acetonitrile solution of the complex, maxima at 523, 372, 362, 273, and 211 nm are present. Assignments of the calculated transitions to the experimental bands are based on criteria of energy and oscillator strength of the calculated transitions. In the description of the electronic transitions, only the main components of the molecular orbitals are taken into consideration. Electronic transitions were calculated with the application of CAM-B3LYP functional using the Coulomb-attenuating method. Figure 6 presents the experimental and calculated electronic spectra of the complex.

The first transition at 523 nm has HOMO → LUMO (94%) character. As the HOMO and LUMO are localized on the d rhenium orbitals with an admixture of π_{Br} this is a ligand field transition. Low-intensity bands with maxima at 372 and 362 nm have the ligand field with contribution of charge-transfer character and the transitions between HOMO-10 → LUMO (52%), HOMO-11 → LUMO (45%), and HOMO-12 → LUMO (50%) are calculated. The band with maximum at 273 nm is attributed to the transitions of ligand–metal and metal–ligand charge transfer with ligand field contribution. The highest energy band with maximum at 211 nm is attributed to the transitions of ligand–ligand charge-transfer type ($\pi_{Ph} \rightarrow \pi^*_{Ph}$ transitions in the PPh_3 ligand). Table 5 presents the calculated transitions for the complex.

In the octahedral symmetry the ground ^3F term splits into $^3T_1$, $^3T_2$, and $^3A_2$ terms which in the lower symmetry (C_{2h}) of the complex split into $^3A_1$, $^3A_2$, $^3B_1$, and $^3B_2$ levels. Based on the electronic spectrum of the complex the ligand field parameters 10 Dq and B are 17 500 cm^{-1} and 547 cm^{-1}, respectively.

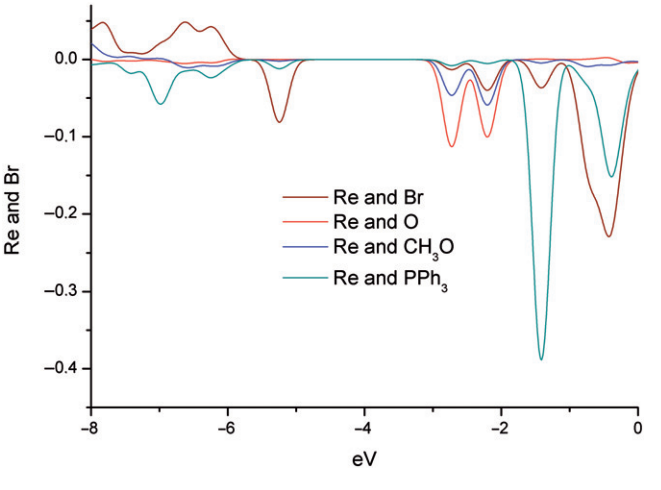

Figure 5. The OPDOS diagram for $[ReBr_2(O)(OCH_3)(PPh_3)_2]$.

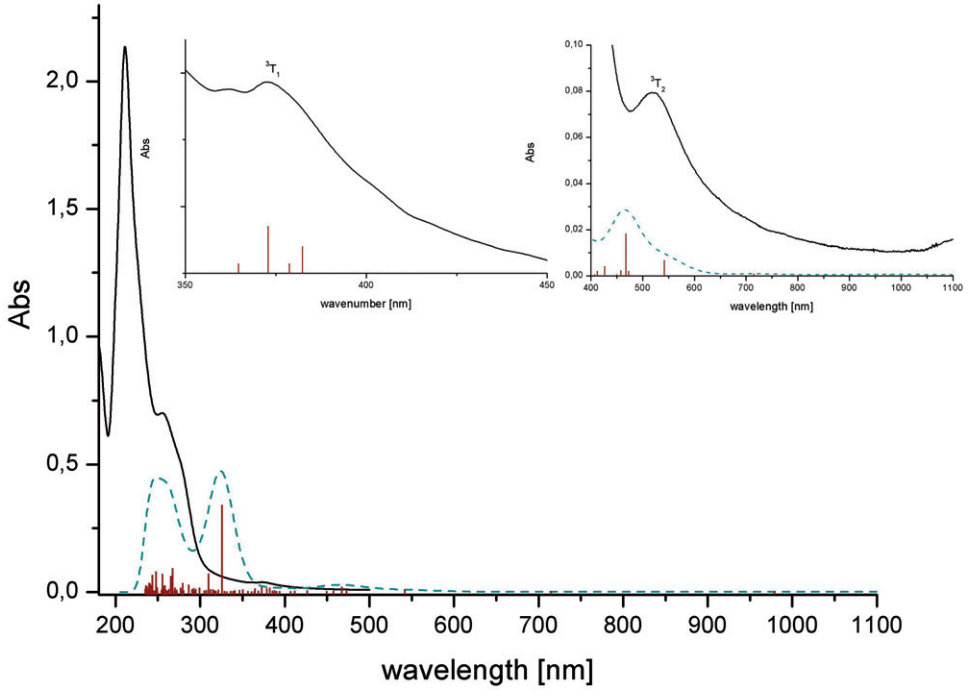

Figure 6. The experimental electronic spectrum of $[ReBr_2(O)(OCH_3)(PPh_3)_2]$ with the calculated transitions.

Table 5. Calculated electronic transitions for $[ReBr_2(O)(OCH_3)(PPh_3)_2]$ with the TDDFT method.

λ (nm)	Contributions	f	Experimental λ (nm)
541.8	HOMO → LUMO (94%)	0.0067	523
472.9	HOMO → L + 1 (93%)	0.0021	–
411.9	H-18 → LUMO (25%); H-15 → LUMO (10%)	0.0020	–
387.8	H-17 → LUMO (16%); H-16 → LUMO (34%)	0.0034	372
372.8	H-20 → LUMO (52%)	0.0007	–
368.7	H-15 → LUMO (17%); H-11 → LUMO (45%)	0.0013	–
363.8	H-18 → LUMO (50%); H-11 → LUMO (14%)	0.0004	362
360.7	H-15 → LUMO (21%); H-13 → LUMO (35%)	0.0023	–
346.7	H-7 → L + 1 (44%); H-5 → L + 1 (17%)	0.0057	–
292.3	H-19 → LUMO (28%); HOMO → L + 5 (41%)	0.0131	–
290.2	HOMO → L + 4 (94%)	0.0080	–
279.2	HOMO → L + 6 (96%)	0.0335	–
276.8	HOMO → L + 7 (86%)	0.0148	273
267.0	H-1 → L + 3 (35%); HOMO → L + 8 (48%)	0.0910	–

Supplementary material

CCDC 815403 contains the supplementary crystallographic data for $[ReBr_2(O)(OCH_3)(PPh_3)_2]$. These data can be obtained free of charge from http://www.ccdc.cam.ac.uk/conts/retrieving.html, or from the Cambridge Crystallographic Data Centre, 12 Union Road, Cambridge CB2 1EZ, UK; Fax: (+44) 1223-336-033; or E-mail: deposit@ccdc.cam.ac.uk.

Acknowledgments

The GAUSSIAN09 calculations were carried out in the Wrocław Centre for Networking and Supercomputing, WCSS, Wrocław, Poland (http://www.wcss.wroc.pl grant number 18). Elemental analyses were performed by Dr Tomasz Radko, Department of Inorganic Chemistry and Technology, Faculty of Chemistry, Silesian University of Technology, 44-100 Gliwice, Poland. Michał Krompiec acknowledges the financial support of the Foundation for Polish Science (START scholarship).

References

[1] A.R. Cowley, J.R. Dilworth, P.S. Donnelly. *Inorg. Chem.*, **42**, 929 (2003).
[2] G. Stöcklin, S.M. Qaim, F. Rösch. *Radiochim. Acta*, **70/71**, 249 (1995).
[3] J.R. Dilworth, S.J. Parrott. *Chem. Soc. Rev.*, **27**, 43 (1998).
[4] W.A. Volkert, T.J. Hoffman. *Chem Rev.*, **99**, 2269 (1999).
[5] E.A. Deutsch, K. Libson, J.L. Vanderheyden. *Technetium and Rhenium in Chemistry and Nuclear Medicine*, Raven Press, New York (1990).
[6] J.H. Espenson. *Coord. Chem. Rev.*, **249**, 329 (2005).
[7] B. Royo, C.C. Romão. *J. Mol. Catal. A: Chem.*, **236**, 107 (2005).
[8] H.Q.N. Gunaratne, M.A. McKervey, S. Feutren, J. Finlay, J. Boyd. *Tetrahedron Lett.*, **39**, 5655 (1998).
[9] Y. Kotani, M. Kamigaito, M. Sawamoto. *Macromolecules*, **33**, 6746 (2000).
[10] R. Mahfouz, E. Al-Frag, M. Rafiq, H. Siddiqui, W.Z. Al-kiali, O. Karama. *Arabian J. Chem.*, **4**, 119 (2011).
[11] D.L. Strand, T. Rein. *J. Organomet. Chem.*, **695**, 2220 (2010).
[12] A.M. Lebuis, C. Roux, L. Beauchamp. *Acta Crystallogr., Sect. C*, **49**, 33 (1993).
[13] A.M. Kirillov, M. Haukka, A.J.L. Pombeiro. *Inorg. Chim. Acta*, **359**, 4421 (2006).
[14] J. Gancheff, C. Kremer, E. Kremer, O.N. Ventura. *J. Mol. Struct. (Theochem)*, **580**, 107 (2002).
[15] M.L. Kuznestov, E.A. Klestova-Nadeeva, A.I. Dement'ev. *J. Mol. Struct. (Theochem)*, **671**, 229 (2004).
[16] M.C. Aragoni, M. Arca, T. Cassano, C. Denotti, F.A. Devillanova, F. Isaia, V. Lippolis, D. Natali, L. Niti, M. Sampietro, R. Tommasi, G. Verani. *Inorg. Chem. Commun.*, **5**, 869 (2002).
[17] P. Romaniello, F. Lelj. *Chem. Phys. Lett.*, **372**, 51 (2003).
[18] P. Norman, P. Cronstrand, J. Ericsson. *Chem. Phys.*, **285**, 207 (2002).
[19] N.P. Johnson, C.J. Lock, G. Wilkinson. *J. Chem. Soc. A*, 1054 (1964).
[20] J. Chatt, J.R. Dilworth, G.J. Leigh, V.P. Gupta. *J. Chem. Soc. A*, 2631 (1971).
[21] M.J. Frisch, G.W. Trucks, H.B. Schlegel, G.E. Scuseria, M.A. Robb, J.R. Cheeseman, G. Scalmani, V. Barone, B. Mennucci, G.A. Petersson, H. Nakatsuji, M. Caricato, X. Li, H.P. Hratchian, A.F. Izmaylov, J. Bloino, G. Zheng, J.L. Sonnenberg, M. Hada, M. Ehara, K. Toyota, R. Fukuda, J. Hasegawa, M. Ishida, T. Nakajima, Y. Honda, O. Kitao, H. Nakai, T. Vreven, J.A. Montgomery, J.J.E. Peralta, F. Ogliaro, M. Bearpark, J.J. Heyd, E. Brothers, K.N. Kudin, V.N. Staroverov, R. Kobayashi, J. Normand, K. Raghavachari, A. Rendell, J.C. Burant, S.S. Iyengar, J. Tomasi, M. Cossi, N. Rega, J.M. Millam, M. Klene, J.E. Knox, J.B. Cross, V. Bakken, C. Adamo, J. Jaramillo, R. Gomperts, R.E. Stratmann, O. Yazyev, A.J. Austin, R. Cammi, C. Pomelli, J.W. Ochterski, R.L. Martin, K. Morokuma, V.G. Zakrzewski, G.A. Voth, P. Salvador, J.J. Dannenberg, S. Dapprich, A.D. Daniels, O. Farkas, J.B. Foresman, J.V. Ortiz, J. Cioslowski, D.J. Fox. *Gaussian 09, Revision A.1*, Gaussian, Inc., Wallingford, CT (2009).
[22] A.D. Becke. *J. Chem. Phys.*, **98**, 5648 (1993).
[23] C. Lee, W. Yang, R.G. Parr. *Phys. Rev. B*, **37**, 785 (1988).
[24] M.E. Casida. In *Recent Developments and Applications of Modern Density Functional Theory, Theoretical and Computational Chemistry*, J.M. Seminario (Ed.), Vol. 4, p. 391, Elsevier, Amsterdam (1996).
[25] T. Yanai, D. Tew, N. Handy. *Chem. Phys. Lett.*, **393**, 51 (2004).
[26] P.J. Hay, W.R. Wadt. *J. Chem. Phys.*, **82**, 299 (1985).
[27] N.M. O'Boyle, A.L. Tenderholt, K.M. Langner. *J. Comp. Chem.*, **29**, 839 (2008).
[28] Stoe & Cie. *X-RED Version 1.18*, STOE & Cie GmbH, Darmstadt, Germany.
[29] G.M. Sheldrick. *Acta Crystallogr., Sect. A*, **46**, 467 (1990).
[30] G.M. Sheldrick. *SHELXL97. Program for the Solution and Refinement of Crystal Structures*, University of Gottingen, Germany (1997).
[31] G.M. Sheldrick. *SHELXTL: Release 4.1 for Siemens Crystallographic Research Systems*, Germany (1990).
[32] B. Machura, M. Wolff, A. Świtlicka, R. Kruszynski, J. Kusz. *Inorg. Chem. Commun.*, **12**, 789 (2009).

[33] K. Nakamoto. *Infrared and Raman Spectra of Inorganic and Coordination Compounds*, 4th Edn, Wiley-Interscience, New York (1986).
[34] B. Machura, A. Switlicka, M. Wolff, J. Kusz, R. Kruszynski. *Polyhedron*, **28**, 3999 (2009).
[35] S. Michalik, J.O. Dzięgielewski, R. Kruszynski. *J. Coord. Chem.*, **58**, 1493 (2005).
[36] E.J. de Souza, A.G. de, A. Fernandes, V.M. Deflon, K.E. Bessler, S.S. Lemos, A.A. Batista, J. Ellena, E.E. Castellano, U. Abram, A. Hagenbach. *J. Braz. Chem. Soc.*, **17**, 1578 (2006).
[37] W.A. Nuguent, J.M. Mayer. *Metal–Ligand Multiple Bonds*, Wiley-Interscience, New York (1988).
[38] B. Machura, R. Kruszyński. *Polyhedron*, **26**, 2957 (2007).
[39] R. Chiozzone, R. González, C. Kremer, G. De Munno, J. Faus. *Inorg. Chim. Acta*, **325**, 203 (2001).
[40] F.H. Allen. *Acta Crystallogr., Sect. B*, **58**, 380 (2002).
[41] G.A. Jeffrey, W. Saenger. *Hydrogen Bonding in Biological Structures*, Springer-Verlag, Berlin and New York (1994).
[42] G.R. Desiraju, T. Steiner. *The Weak Hydrogen Bond in Structural Chemistry and Biology*, Oxford University Press, Oxford (1999).
[43] L. Wei, J. Babich, J. Zubieta. *Inorg. Chim. Acta*, **358**, 2413 (2005).
[44] D. Nunes, A. Domingos, A. Paulo, L. Patricio, I. Santos, M.F.N.N. Carvalho, A.J.L. Pombeiro. *Inorg. Chim. Acta*, **271**, 65 (1998).